ARTICLES

The POT1–TPP1 telomere complex is a telomerase processivity factor

Feng Wang[1], Elaine R. Podell[2], Arthur J. Zaug[2], Yuting Yang[1], Paul Baciu[1], Thomas R. Cech[2] & Ming Lei[1]

Telomeres were originally defined as chromosome caps that prevent the natural ends of linear chromosomes from undergoing deleterious degradation and fusion events. POT1 (protection of telomeres) protein binds the single-stranded G-rich DNA overhangs at human chromosome ends and suppresses unwanted DNA repair activities. TPP1 is a previously identified binding partner of POT1 that has been proposed to form part of a six-protein shelterin complex at telomeres. Here, the crystal structure of a domain of human TPP1 reveals an oligonucleotide/oligosaccharide-binding fold that is structurally similar to the β-subunit of the telomere end-binding protein of a ciliated protozoan, suggesting that TPP1 is the missing β-subunit of human POT1 protein. Telomeric DNA end-binding proteins have generally been found to inhibit rather than stimulate the action of the chromosome end-replicating enzyme, telomerase. In contrast, we find that TPP1 and POT1 form a complex with telomeric DNA that increases the activity and processivity of the human telomerase core enzyme. We propose that POT1–TPP1 switches from inhibiting telomerase access to the telomere, as a component of shelterin, to serving as a processivity factor for telomerase during telomere extension.

Telomeres, the specialized DNA–protein complexes found at the termini of all linear eukaryotic chromosomes, protect chromosomes from degradation and end-to-end fusion[1]. Telomeric DNA typically consists of tandem repeats of a short G-rich sequence oriented 5′ to 3′ towards the chromosome terminus, with the G-rich strand extending beyond its complement to form a 3′ overhang. In most eukaryotes, telomere length is maintained by telomerase, a specialized reverse transcriptase that adds telomeric DNA to the 3′ ends of chromosomes to ensure complete genome replication[2]. Telomerase is strongly upregulated in most cancer cells and has been studied as a plausible anti-cancer target[3].

A six-protein complex is thought to protect the telomeres of human chromosomes. TRF1 and TRF2 directly bind double-stranded telomeric DNA[4,5], POT1 directly binds the single-stranded 3′ extension at the chromosome end[6–11], and these are bridged through protein–protein interactions involving TIN2 and TPP1 (refs 12–19). The sixth protein, RAP1, binds mostly to TRF2 (refs 18, 20). Two functions have been proposed for this complex: protecting the natural chromosome end from being mistaken for a broken end and being subjected to DNA repair, and negative regulation of telomerase by sequestration of its telomeric DNA substrate. Both functions of this complex are captured by the name shelterin[21].

Because POT1–TPP1 has been viewed as a structural component of the telomere, we were surprised to find that it increases both the activity and processivity of core telomerase. This is the first protein complex shown to substantially activate telomerase processivity. The crystal structure of TPP1 shows high structural similarity to the β-subunit of TEBP (telomere end-binding protein) from *Oxytricha nova*, a ciliated protozoan[22–24]. Because POT1 is the human homologue of TEBPα[6,7,10,25], it now appears that capping of telomeres by a TEBPα–β dimer is more conserved evolutionarily than had been expected.

TPP1 and POT1 form ternary complexes with ssDNA

Recombinant human TPP1 protein with an N-terminal deletion, TPP1(90−544) (Fig. 1a), was overexpressed and purified from *Escherichia coli*. TPP1(90−544) was chosen because the 87 N-terminal residues of TPP1 are functionally dispensable in human cells[12–14] and are not conserved among TPP1 proteins of different organisms[12,13]. For simplicity, we hereafter use TPP1 to represent TPP1(90−544) unless stated otherwise.

An 18-nucleotide single-stranded telomeric DNA (primer a, $(TTAGGG)_3$) was incubated with increasing amounts of TPP1 with or without POT1, and binding was analysed by electrophoretic mobility shift assay (EMSA). POT1 protein bound to the DNA, whereas TPP1 on its own did not, even at a high protein concentration (375 nM) (Fig. 1b, lanes 1–5). When TPP1 was added to the POT1–DNA mixture, however, an additional complex formed that migrated above the POT1–DNA complex (Fig. 1b, lanes 6–11). By two criteria, this more slowly migrating complex contained TPP1. First, two size variants of TPP1, both of which contain the POT1-binding domain (Fig. 1a), produced electrophoretically distinct complexes (Fig. 1c). Second, addition of an anti-His antibody confirmed that the slower complex contained His-tagged TPP1 (Fig. 1d). The amount of DNA in the ternary complex was increased compared with the amount of DNA bound to POT1 alone (compare lanes 5 and 11 in Fig. 1b), suggesting higher affinity.

The equilibrium dissociation constants (K_d) of the protein complexes with various telomeric single-stranded (ss)DNAs were determined. Primer a (Fig. 2a) bound POT1 with a K_d of 26 nM, and the stability of this complex was increased sixfold by addition of TPP1 (Supplementary Fig. 1). Primers a5 and a3 (Fig. 2a) contain single-nucleotide substitutions that force POT1 to bind either to a 5′ site (corresponding to an internal site on a long telomeric G-overhang) or to a 3′-proximal site (corresponding to end-capping)[26]. The POT1–TPP1 complex showed a substantial preference for 3′-end binding ($K_d = 0.7$ versus 7.4 nM; compare circles in Fig. 2b, c). Notably, the dissociation constant of POT1–a5 is also tenfold higher than that of POT1–a3 (8.3 versus 89 nM) (compare triangles in Fig. 2b, c), suggesting that the 3′ end preference of the POT1–TPP1 complex is mainly dictated by POT1. Measurements of the

[1]Department of Biological Chemistry, University of Michigan Medical School, MSRBIII 5301D, 1150 W. Medical Center Drive, Ann Arbor, Michigan 48109, USA. [2]Howard Hughes Medical Institute, Department of Chemistry and Biochemistry, University of Colorado, Boulder, Colorado 80309, USA.

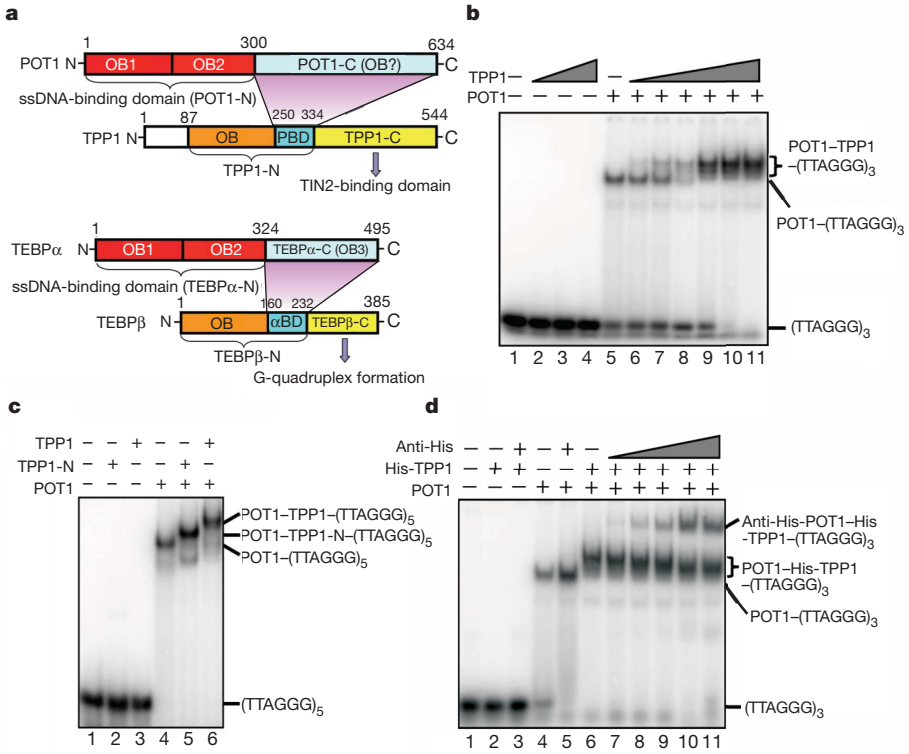

Figure 1 | TPP1 binds to the POT1–ssDNA complex and enhances the POT1–ssDNA interaction. **a**, Human POT1–TPP1 and *O. nova* TEBPα–β complexes share similar domain organization. In POT1 and TEBPα, the N-terminal ssDNA-binding domains are coloured in red, and the C-terminal TPP1/TEBPβ-binding domains are in light blue. In TPP1 and TEBPβ, the N-terminal OB folds are in orange, the central α-subunit-binding region (PBD in TPP1 and αBD in TEBPβ) is in cyan, and the C-terminal domains are in yellow. Numbers indicate amino acid positions at the boundaries of various subdivisions. **b**, TPP1 requires POT1 in order to interact stably with telomeric DNA. Primer a (50 nM) was incubated with increasing amounts of TPP1 (2, 10 and 50 nM in lanes 2–4, 2–100 nM in lanes 6–11) in the absence or presence of 150 nM POT1. **c**, Both TPP1 and TPP1-N generate super-shifted species but with different mobility; use of a longer primer enhanced the separation. **d**, The addition of anti-His antibody TPP1 detected the existence of His-tagged TPP1 in the slower migrating complex.

kinetic stabilities of the various complexes confirmed that the off rate of the POT1–DNA complex was decreased by addition of equimolar TPP1 (Supplementary Fig. 1). Furthermore, the complexes with a3 were kinetically about tenfold more stable than those with a5 (Supplementary Fig. 1). Taken together, these data indicate two POT1–TPP1 binding modes on telomeric DNA, a lower affinity one at internal sequences and a higher affinity one at the 3′ end.

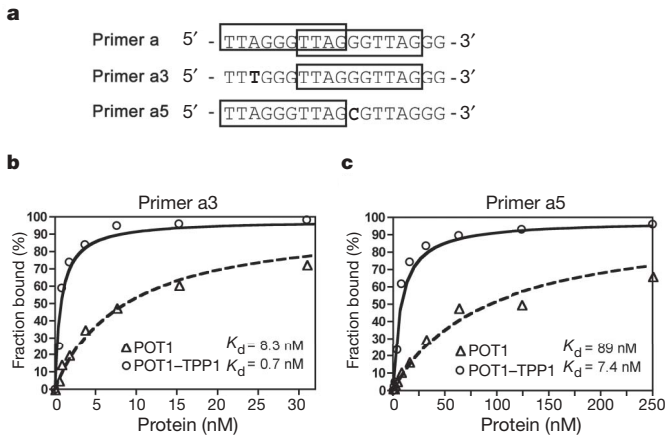

Figure 2 | The POT1–TPP1 complex binds to the single-stranded telomeric overhang with 3′ end preference. **a**, Sequences of primers a, a5 and a3. The bold letters are the point mutations. The POT1-binding sites are denoted by boxes[26]. **b**, **c**, Equilibrium binding curves for primers a3 (**b**) and a5 (**c**) binding to POT1 and the POT1–TPP1 complex. The solid and dashed lines represent theoretical binding curves fit to the data for POT1 and POT1–TPP1, respectively. The calculated equilibrium dissociation constant (K_d) values are indicated. The binding curves and K_d values for primers a, b and hT10 (TTAGGGTTAG) are shown in Supplementary Fig. 1.

Structural conservation between TPP1 and TEBPβ

Functional and structural studies have established that POT1 is the human homologue of the *O. nova* TEBP α-subunit[6,7,10,25]. Although there has been no report of a TEBP β-subunit in any organism besides *O. nova* and a related ciliate, *Stylonychia mytilis*[27], the DNA-binding properties of POT1–TPP1 closely resembled those of *O. nova* TEBPα–β[28], consistent with TPP1 being the human homologue of TEBPβ. In addition, their domain organizations revealed clear similarities (Fig. 1a). First, both TPP1 and TEBPβ use a central region (PBD in TPP1 and αBD in TEBPβ) to interact with the carboxy-terminal domains of their binding partners (POT1-C and TEBPα-C). Second, primary sequence analysis of the N-terminal domain of TPP1 (residues 90–250) predicted a secondary structure pattern of α-**β**-**β**-**β**-**α**-**β**-**β**-α (data not shown), where the bold region is characteristic of oligonucleotide/oligosaccharide-binding (OB) folds found in many telomere-binding proteins including TEBPβ[10,23]. Third, the C-terminal domains of both TPP1 and TEBPβ (TPP1-C and TEBPβ-C) are not involved in the interaction with the α-subunits (POT1 and TEBPα) and have evolved to have distinct functions[13,14,18,29,30] (Fig. 1a).

For crystallization studies, we first purified the N-terminal fragment TPP1-N (Fig. 1a), which can interact with POT1 and would correspond to the TEBPβ fragment in the TEBPα–β–ssDNA crystal structure[23]. However, TPP1-N was unstable by itself. Limited proteolysis and matrix-assisted laser desorption/ionization (MALDI) mass spectrometry identified a protease-resistant core domain of TPP1-N containing residues 90–260 (Supplementary Fig. 2); this domain corresponds to the predicted OB fold (Fig. 1a).

Recombinant TPP1(90–250) expressed from *E. coli* was crystallized, and the structure was solved by single anomalous dispersion (SAD) and refined to a resolution of 2.7 Å (Supplementary Table 1). The final model contains residues 90–243 (Fig. 3a).

The structure of TPP1(90–250) reveals a typical OB-fold architecture comprising a highly curved five-stranded β-barrel (Fig. 3a)[31,32]. Hereafter, we will refer to TPP1(90–250) as TPP1-OB (Fig. 1a). An unbiased search for structurally homologous proteins using Dali[33] revealed that the structure of TPP1-OB is most similar to that of the OB fold of the *O. nova* TEBP β-subunit[23]. The two structures can be superimposed with a root-mean-square deviation of 2.0 Å in the positions of 144 equivalent Cα atoms (Fig. 3b). Notably, this structurally conserved region includes not only the central β-barrel, but also three peripheral α-helices, suggesting that TPP1 and TEBPβ are homologous proteins (Fig. 3b); other OB folds, such as that of TEBPα, are more distantly related (Fig. 3c). In addition to the overall structural similarity, the OB folds of TPP1 and TEBPβ share several unique features. First, the loop connecting β5 and αC (L_{5C}), unlike in the OB folds of POT1 and TEBPα, adopts an extended conformation and packs across one side of the β-barrel, forcing helix αC to cap the bottom of the barrel (Fig. 3b). Second, helix αB is in a modified position, rotated almost 90° relative to the orientation normally observed in OB folds. Taken together, these structural similarities strongly support the notion that TPP1 is the human homologue of *O. nova* TEBPβ. Given that TPP1 has been identified in many other eukaryotes[12,13], TPP1/TEBPβ may be an evolutionarily conserved telomere protein.

Despite the high degree of structural conservation, the sequences of OB folds of TPP1 and TEBPβ are markedly divergent and share only 11% identity (Supplementary Fig. 3). Significant sequence and structural variation is particularly evident in the connecting loop regions. TPP1-OB has a very long loop (20 residues), L_{12}, between strands β1 and β2, which packs on helix αA and covers one end of the barrel (Fig. 3a, b). In contrast, strands β1 and β2 of TEBPβ are connected by a short two-residue turn (Fig. 3b). These marked variances in the loop regions explain the failure to detect the similarity between these OB folds by bioinformatics.

POT1–TPP1 is a telomerase processivity factor

We investigated the ability of telomerase to extend the POT1–TPP1–ssDNA ternary complex, expecting some inhibition consistent with the shelterin model[21]. Human core telomerase was reconstituted *in vitro* and immunopurified via the haemagglutinin (HA) tag on the telomerase catalytic subunit (TERT). Primer a5 has a single-nucleotide mutation that forces POT1 to bind to its 5′ end (Fig. 2a), leaving a telomerase-extendible 3′ tail[26]. Addition of POT1 and TPP1 to primer a5 markedly increased the telomerase product size distribution. Primer a5 was extended via more than 30 cycles of template copying (Fig. 4a, lane 4), whereas in the absence of the POT1–TPP1 complex, the first three cycles accounted for most of the extension (lane 1). Under conditions of vast primer excess, longer extension products result from processive extension, not from rebinding of previously extended products[34]. We confirmed that this condition still pertained in the case of the ternary complexes by showing that the extension was independent of concentration over a 2,000-fold range (Supplementary Fig. 4).

These data emphasize the longer extension products, because ^{32}P-GMP incorporation increases with product size. Quantification showed that POT1–TPP1 provided a threefold increase in activity (Fig. 4b) and, after dividing each product by the amount of GMP incorporated, a fourfold increase in processivity (Fig. 4c). $R_{1/2}$, the number of repeats synthesized before half of the chains have dissociated, increased from 0.78 repeats with DNA primer a5 to 3.3 repeats with the POT1–TPP1–DNA complex. Because this fourfold increase in processivity is cumulative, it has a very large effect on the production of longer products (see double-headed arrows in Fig. 4c–e). POT1 by itself produced a more modest stimulation of processivity, consistent with earlier results[26], and TPP1 by itself had a similar effect (Fig. 4c–e).

The increase in telomerase processivity with the POT1–TPP1 complex was unexpected, and we were concerned that it might be due to a small molecule accompanying the protein. However, when we fractionated TPP1 by gel filtration chromatography, the processivity activity clearly co-migrated with the main protein peak (Supplementary Fig. 5), indicating that the enhanced processivity was TPP1-specific.

The effects of POT1 and TPP1 were even more dramatic with other DNA primers. Primer a3 binds POT1 mainly at its 3′ end (Fig. 2a), as does primer b ($(GGTTAG)_3$)[26]. As expected, the addition of POT1 almost completely blocked the extension of these primers (Fig. 4a, lanes 6 and 10). When TPP1 was also added, however, telomere extension was rescued and processivity was increased five- to sixfold (Fig. 4a, lanes 8 and 12; see also Fig. 4d, e). To test the possibility that TPP1 induced sliding of POT1 from the preferred 3′ binding site to the 5′ site, we mapped the position of the leading edge of the POT1–TPP1 complex on the DNA using snake-venom phosphodiesterase I, which degrades ssDNA exonucleolytically from the 3′ end. Complexes of primer a3 or primer a with the POT1–TPP1 heterodimer showed that the protein mostly occupied the DNA 3′ end, with a local change in accessibility relative to the POT1–DNA complexes where the 3′ end of the DNA protrudes from the protein (Supplementary Fig. 6). Although TPP1 did not relocate the bulk of POT1 to an internal site on the DNA, we propose that the proteins are in fact binding internally in a minority of the complexes[26]; the resulting 3′ overhang is then extended by telomerase with the enhanced processivity characteristic of POT1–TPP1 complexes.

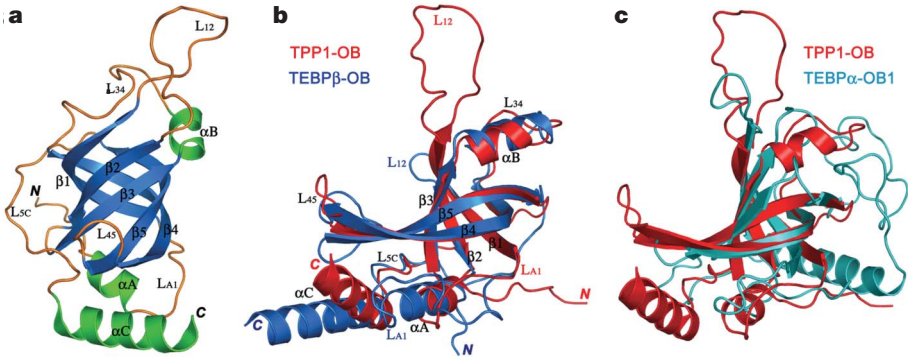

Figure 3 | The crystal structure of TPP1-OB indicates that TPP1 is the homologue of *O. nova* TEBPβ. **a**, Ribbon diagram of TPP1-OB with β-strands coloured in blue, α-helices green, and loops orange. The secondary structure elements are labelled. **b**, Superposition of TPP1-OB on the crystal structure of the OB fold of TEBPβ[23]. TPP1 is in red and TEBPβ in blue. **c**, Superposition of TPP1-OB on the crystal structure of the first OB fold of TEBPα[23]. TPP1 is in red and TEBPα in cyan. Figures were generated by using the program Pymol (http://pymol.sourceforge.net).

Primer AGGG-a (AGGG(TTAGGG)$_3$) has four blocks of GGG and therefore folds into Hoogsteen base-paired G-quadruplex structures, which are inhibitory for telomerase extension (Fig. 4a, lane 13)[35]. POT1 can trap an open form of this DNA, allowing telomerase extension[35] (lane 14). TPP1 by itself (lane 15) gave the typical twofold increase in telomerase activity seen with all the primers (Fig. 4b), but telomerase still stalled after every nucleotide added to the G-quadruplex. POT1–TPP1 again stimulated highly processive extension by telomerase (lane 16).

We next asked whether the enhanced telomerase processivity and activity were dependent on the POT1–TPP1 interaction by using a panel of POT1 and TPP1 deletion mutant proteins. POT1-N, which lacks the TPP1 interaction domain, and TPP1-OB, which lacks the POT1 interaction domain, both failed to endow telomerase with increased processivity and activity (Supplementary Fig. 7). Only when both proteins had intact interaction domains was the processivity greatly stimulated (Supplementary Fig. 7), confirming the important role of the POT1–TPP1 interaction in this activity. The purified POT1 interaction domain of TPP1, TPP1-PBD, was insufficient to activate telomerase in the presence of POT1 (Supplementary Fig. 8).

Discussion

E. coli DNA polymerase achieves high processivity by means of an accessory protein that serves as a 'sliding clamp', encircling the DNA and preventing dissociation[36]. By analogy, the POT1–TPP1 complex might move with telomerase, binding the DNA just upstream from its 3′ end and inhibiting dissociation. Given the DNA sequence-specificity of POT1–TPP1 binding, the protein would not slide continuously along the DNA but would ratchet in 6- or 12-nucleotide steps. On the other hand, ssDNA is intrinsically much more flexible than double-stranded (ds)DNA. Thus, a clamp would not need to slide or ratchet to keep the ssDNA associated with telomerase, but could instead remain fixed while the newly synthesized telomeric repeats formed a larger and larger protruding loop. Another question for future research is whether a single POT1–TPP1 complex clamp is sufficient for increased processivity, or whether the proteins must coat the elongating telomeric DNA.

In normal human somatic cells that lack telomerase, telomeres shrink by about 30–100 base pairs per replication cycle[37]. This provides a plausible estimate for the amount of DNA synthesized by telomerase at each chromosome end, and is similar to more direct measurements in yeast[38]. Whether such extension is processive or distributive *in vivo* is unknown. However, we note that the telomerase processivity achieved here in the presence of POT1–TPP1 is around four repeats or 24 nucleotides, which would mean that one or a few rounds of telomerase extension per cell cycle would be sufficient to maintain human telomeres.

Given that POT1 and TPP1 are components of a negative feedback loop of telomere length control[11–14], we were surprised to find that the

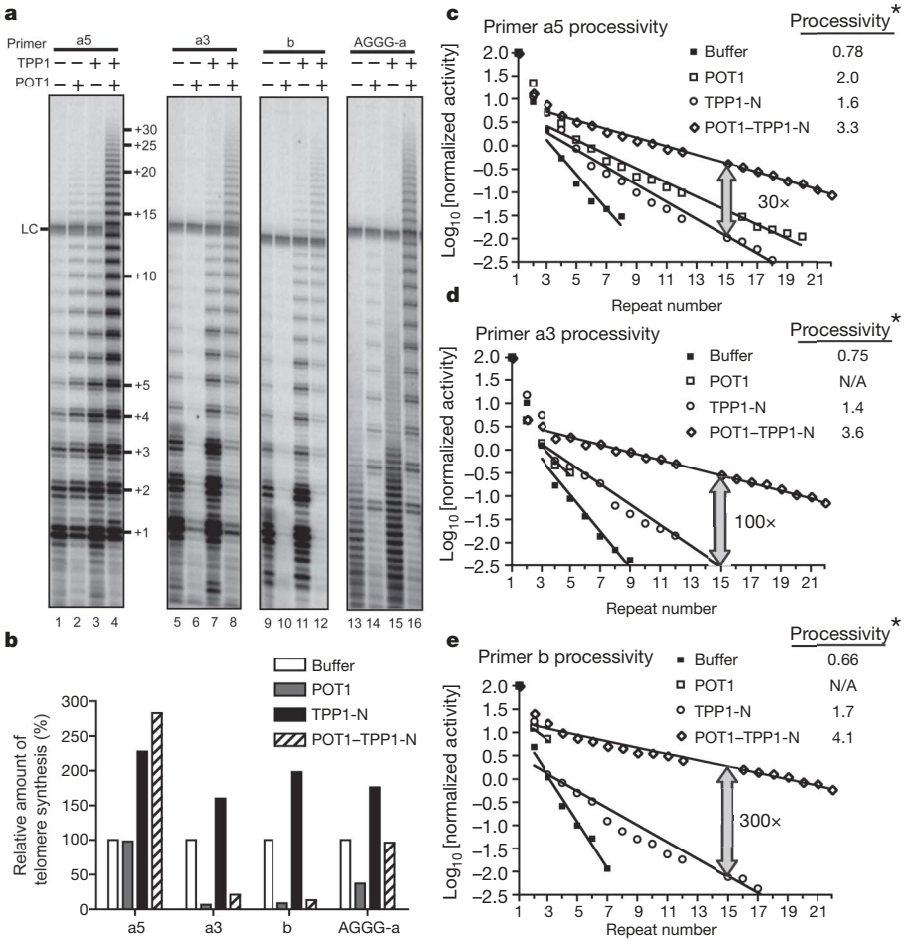

Figure 4 | The POT1–TPP1 complex functions as a telomerase processivity factor. a, Direct telomerase activity assays[34] were performed with 100 nM primer a5 (lanes 1–4), a3 (lanes 5–8), b (lanes 9–12), or AGGG-a (lanes 13–16) in the presence of a saturating concentration of POT1, TPP1, or POT1–TPP1. Reaction products were then analysed by gel electrophoresis (LC, loading control). Three independent sets of experiments gave equivalent results. **b**, Quantification of total DNA synthesis relative to synthesis in the presence of protein buffer alone. **c**–**e**, Activity in each repeat shown in **a** was measured, corrected for the number of radiolabelled nucleotides incorporated, and then plotted. *Processivity = $R_{1/2} = -\ln 2/(2.303k)$, where k is the slope and $R_{1/2}$ is the number of repeats synthesized before half of the chains have dissociated, analogous to $t_{1/2}$ in radioactive decay.

POT1–TPP1 complex can also function as a positive telomerase processivity factor. We propose a three-state model of telomere length regulation that can reconcile the two apparently opposite functions of POT1–TPP1. (1) When POT1–TPP1 covers the 3′ terminus of the G-overhang, it sequesters the telomere and prevents binding of telomerase. (2) POT1–TPP1 is removed from its high-affinity 3′ binding site by an unidentified mechanism, which might, for example, involve post-translational modification and disruption of the shelterin complex. (3) The POT1–TPP1 complex then serves as a telomerase processivity factor during telomere extension. As the telomere is elongated and reaches a certain threshold, the newly synthesized repeats bind shelterin complexes, the 3′ end of the overhang is re-bound by POT1–TPP1, and further telomerase extension is inhibited (back to state 1). Further work will be needed to understand how switching between such telomere and telomerase complexes is achieved and regulated *in vivo*.

METHODS

Details of recombinant protein cloning, expression and purification can be found in Supplementary Methods. Telomeric ssDNAs used in the DNA-binding assay were purchased from IDT and Invitrogen and 5′-end-labelled using polynucleotide kinase. Protein binding proceeded for 1 h at room temperature in 90 mM NaCl, 50 mM Tris-HCl, pH 8.0, 6 mM dithiothreitol and 5% glycerol, followed by EMSA on native 6% polyacrylamide gels[10]. For *in vitro* telomerase activity assays[26], C-terminal HA-tagged human TERT was expressed from phTERT-HA2 and hTR from phTR[34] using the TnT quick-coupled transcription/translation system (Promega), and the reconstituted core telomerase was affinity-purified on anti-HA F7-agarose beads (Santa Cruz Biotechnology)[26]. Details of crystallization, data collection and structure determination of TPP1-OB can be found in Supplementary Methods.

Received 17 August; accepted 17 November 2006.
Published online 21 January 2007.

1. Blackburn, E. H. Switching and signaling at the telomere. *Cell* **106,** 661–673 (2001).
2. Cech, T. R. Beginning to understand the end of the chromosome. *Cell* **116,** 273–279 (2004).
3. Shay, J. W. & Wright, W. E. Telomerase: a target for cancer therapeutics. *Cancer Cell* **2,** 257–265 (2002).
4. Chong, L. *et al.* A human telomeric protein. *Science* **270,** 1663–1667 (1995).
5. Broccoli, D., Smogorzewska, A., Chong, L. & de Lange, T. Human telomeres contain two distinct Myb-related proteins, TRF1 and TRF2. *Nature Genet.* **17,** 231–235 (1997).
6. Baumann, P. & Cech, T. R. Pot1, the putative telomere end-binding protein in fission yeast and humans. *Science* **292,** 1171–1175 (2001).
7. Baumann, P., Podell, E. & Cech, T. R. Human Pot1 (protection of telomeres) protein: cytolocalization, gene structure, and alternative splicing. *Mol. Cell. Biol.* **22,** 8079–8087 (2002).
8. Hockemeyer, D., Daniels, J. P., Takai, H. & de Lange, T. Recent expansion of the telomeric complex in rodents: Two distinct POT1 proteins protect mouse telomeres. *Cell* **126,** 63–77 (2006).
9. Wu, L. *et al.* Pot1 deficiency initiates DNA damage checkpoint activation and aberrant homologous recombination at telomeres. *Cell* **126,** 49–62 (2006).
10. Lei, M., Podell, E. R. & Cech, T. R. Structure of human POT1 bound to telomeric single-stranded DNA provides a model for chromosome end-protection. *Nature Struct. Mol. Biol.* **11,** 1223–1229 (2004).
11. Loayza, D. & de Lange, T. POT1 as a terminal transducer of TRF1 telomere length control. *Nature* **423,** 1013–1018 (2003).
12. Ye, J. Z. *et al.* POT1-interacting protein PIP1: a telomere length regulator that recruits POT1 to the TIN2/TRF1 complex. *Genes Dev.* **18,** 1649–1654 (2004).
13. Liu, D. *et al.* PTOP interacts with POT1 and regulates its localization to telomeres. *Nature Cell Biol.* **6,** 673–680 (2004).
14. Houghtaling, B. R., Cuttonaro, L., Chang, W. & Smith, S. A dynamic molecular link between the telomere length regulator TRF1 and the chromosome end protector TRF2. *Curr. Biol.* **14,** 1621–1631 (2004).
15. Kim, S. H., Kaminker, P. & Campisi, J. TIN2, a new regulator of telomere length in human cells. *Nature Genet.* **23,** 405–412 (1999).
16. Liu, D. O'connor, M. S., Qin, J. & Songyang, Z. Telosome, a mammalian telomere-associated complex formed by multiple telomeric proteins. *J. Biol. Chem.* **279,** 51338–51342 (2004).
17. Ye, J. Z. *et al.* TIN2 binds TRF1 and TRF2 simultaneously and stabilizes the TRF2 complex on telomeres. *J. Biol. Chem.* **279,** 47264–47271 (2004).
18. O'Connor, M. S., Safari, A., Xin, H., Liu, D. & Songyang, Z. A critical role for TPP1 and TIN2 interaction in high-order telomeric complex assembly. *Proc. Natl Acad. Sci. USA* **103,** 11874–11879 (2006).
19. Kim, S. H. *et al.* TIN2 mediates functions of TRF2 at human telomeres. *J. Biol. Chem.* **279,** 43799–43804 (2004).
20. Li, B., Oestreich, S. & de Lange, T. Identification of human Rap1: implications for telomere evolution. *Cell* **101,** 471–483 (2000).
21. de Lange, T. Shelterin: the protein complex that shapes and safeguards human telomeres. *Genes Dev.* **19,** 2100–2110 (2005).
22. Hicke, B. J., Celander, D. W., MacDonald, G. H., Price, C. M. & Cech, T. R. Two versions of the gene encoding the 41-kilodalton subunit of the telomere binding protein of *Oxytricha nova*. *Proc. Natl Acad. Sci. USA* **87,** 1481–1485 (1990).
23. Horvath, M. P., Schweiker, V. L., Bevilacqua, J. M., Ruggles, J. A. & Schultz, S. C. Crystal structure of the *Oxytricha nova* telomere end binding protein complexed with single strand DNA. *Cell* **95,** 963–974 (1998).
24. Gray, J. T., Celander, D. W., Price, C. M. & Cech, T. R. Cloning and expression of genes for the *Oxytricha* telomere-binding protein: specific subunit interactions in the telomeric complex. *Cell* **67,** 807–814 (1991).
25. Loayza, D., Parsons, H., Donigian, J., Hoke, K. & de Lange, T. DNA binding features of human POT1: a nonamer 5′-TAGGGTTAG-3′ minimal binding site, sequence specificity, and internal binding to multimeric sites. *J. Biol. Chem.* **279,** 13241–13248 (2004).
26. Lei, M., Zaug, A. J., Podell, E. R. & Cech, T. R. Switching human telomerase on and off with hPOT1 protein *in vitro*. *J. Biol. Chem.* **280,** 20449–20456 (2005).
27. Fang, G. W. & Cech, T. R. Molecular cloning of telomere-binding protein genes from *Stylonychia mytilis*. *Nucleic Acids Res.* **19,** 5515–5518 (1991).
28. Fang, G., Gray, J. T. & Cech, T. R. *Oxytricha* telomere-binding protein: separable DNA-binding and dimerization domains of the α-subunit. *Genes Dev.* **7,** 870–882 (1993).
29. Fang, G. & Cech, T. R. The β subunit of *Oxytricha* telomere-binding protein promotes G-quartet formation by telomeric DNA. *Cell* **74,** 875–885 (1993).
30. Paeschke, K., Simonsson, T., Postberg, J., Rhodes, D. & Lipps, H. J. Telomere end-binding proteins control the formation of G-quadruplex DNA structures *in vivo*. *Nature Struct. Mol. Biol.* **12,** 847–854 (2005).
31. Dietmann, S. & Holm, L. Identification of homology in protein structure classification. *Nature Struct. Biol.* **8,** 953–957 (2001).
32. Theobald, D. L., Mitton-Fry, R. M. & Wuttke, D. S. Nucleic acid recognition by OB-fold proteins. *Annu. Rev. Biophys. Biomol. Struct.* **32,** 115–133 (2003).
33. Holm, L. & Sander, C. Database algorithm for generating protein backbone and side-chain co-ordinates from a Cα trace application to model building and detection of co-ordinate errors. *J. Mol. Biol.* **218,** 183–194 (1991).
34. Chen, J. L. & Greider, C. W. Determinants in mammalian telomerase RNA that mediate enzyme processivity and cross-species incompatibility. *EMBO J.* **22,** 304–314 (2003).
35. Zaug, A. J., Podell, E. R. & Cech, T. R. Human POT1 disrupts telomeric G-quadruplexes allowing telomerase extension *in vitro*. *Proc. Natl Acad. Sci. USA* **102,** 10864–10869 (2005).
36. Kuriyan, J. & O'Donnell, M. Sliding clamps of DNA polymerases. *J. Mol. Biol.* **234,** 915–925 (1993).
37. Counter, C. M. *et al.* Telomere shortening associated with chromosome instability is arrested in immortal cells which express telomerase activity. *EMBO J.* **11,** 1921–1929 (1992).
38. Teixeira, M. T., Arneric, M., Sperisen, P. & Lingner, J. Telomere length homeostasis is achieved via a switch between telomerase-extendible and -nonextendible states. *Cell* **117,** 323–335 (2004).

Supplementary Information is linked to the online version of the paper at www.nature.com/nature.

Acknowledgements We thank Y. Chen and K. Wan for help at various stages of the project; N. F. Lue for the His-SUMO protein expression vector; Z. Songyang and T. de Lange for TPP1 cDNA; D. Yoder of beamline 23-ID at APS for assistance with data collection; and J. L. Chen and C. W. Greider for the human TERT and TER plasmids. Work in the laboratory of M.L. is supported by the American Cancer Society and the Sidney Kimmel Foundation. E.R.P., A.J.Z. and T.R.C. are supported by the Howard Hughes Medical Institute.

Author Contributions F.W. is responsible for the bulk of the experiments; Y.Y. for structural determination of TPP1-OB; P.B. for crystallization of TPP1-OB; E.R.P. and A.J.Z. for the telomerase activity assays and some of the EMSA experiments; and T.R.C. and M.L. contributed to overall design and interpretation of the studies.

Author Information The atomic coordinates and structure factors of TPP1-OB have been deposited in the RCSB Protein Data Bank with accession code 2I46. Reprints and permissions information is available at www.nature.com/reprints. The authors declare no competing financial interests. Correspondence and requests for materials should be addressed to M.L. (leim@umich.edu).